Proceedings of the XVII ECSMGE-2019
Geotechnical Engineering foundation of the future
ISBN 978-9935-9436-1-3

doi: 10.32075/17ECSMGE-2019-0949

XVII European Conference
ECSMGE 2019
Reykjavik
on Soil Mechanics
and Geotechnical Engineering

Evaluation of landslide yielding sediments by using multi-temporal high resolution topographies

Bilan sédimentaire de glissements de terrain à l'aide de topographie haute résolution multi-temporelle engendrée par photogrammétrie

C.M. Tseng
Chang Jung Christian University, Tainan, Taiwan (*R.O.C.*)

K.J. Chang
National Taipei University of Technology, Taipei, Taiwan (*R.O.C.*)

Y.S. Chen
Disaster Prevention Research Center, National Cheng Kung University, Tainan, Taiwan (*R.O.C.*)

C.H. Wang, C.C. Li
Soil and Water Conservation Bureau, Council of Agriculture, Nanto, Taiwan (*R.O.C.*)

ABSTRACT: In this study, we studied and monitored a watershed (Pu-tun-pu-nas) with an area of 7 km^2 in southern Taiwan which was seriously affected by the major typhoon Morakot in 2009,. This typhoon brought extreme and long duration rainfall, for instance the cumulated rainfall around the study area was approximately 2,425 mm, and consequently caused severe landslides and debris flows. So after the typhoon Morakot, a large amount of landslide yielding materials had been reactivated resulted in active debris flows during recent years. The purpose of this study is to investigate the sediment budgets related to landslides and debris flows after the typhoon Morakot by using the difference of High Resolution DTM (DoD) method to perform subtraction on the DTMs before and after typhoons. To perform this study we acquired three DTMs generated by the aerial images taken by Unmanned Aerial Vehicle (UAV) and Airborne Digital Sensors (ADS) between 2010 to 2015. The results of this study provides not only geomatics and GIS datasets to monitor the terrassic evolution but also essential geomorphological key information to optimize the hazard mitigation planning.

RÉSUMÉ: Le typhon Morakot (2009) a entraîné des précipitations extrêmes et de longue durée. Un bassin versant d'une superficie de 7 km^2 situé dans le sud de Taïwan (Pu-tun-pu-nas), a recu des précipitations cumulées supérieure à 2.4m provoquant de graves glissements de terrain et des coulées de débris. Ce bassin versant a été choisi pour étudier l'évolution à postériori de la grande quantité de matériaux et des flux de débris actifs résultant de cette érosion. Le but de cette étude est donc d'étudier localement les bilans sédimentaires liés aux glissements de terrain et aux coulées de débris après le typhon Morakot en utilisant la méthode des différences d'altitude obtenues a partir de MNT Haute résolution (DoD) en effectuant une soustraction sur les MNT avant et après le passage du typhon. Au cours de cette étude trois MNT ont été produit a partir des images aériennes prises par les véhicules aériens sans pilote (UAV) et les capteurs numériques aéroportés (ADS) entre 2010 et 2015. Les résultats de cette étude fournissent non seulement une solide base de données géomatique et de SIG permettant de mieux comprendre l'evolution glissements de terrains et des terrasses alluviales et leurs risques afférants et apporte aussi des information essentielles pour la planification de l'atténuation des risques naturels.
Keywords: Sediment yielding; Landslide; Digital terrain model; Unmanned Aerial Vehicle

1 INTRODUCTION

Approximately 75% of Taiwan's land area consists of hillsides with geological fractures and steep slopes, with an average annual precipitation of 2,506 mm, of which 80% occurs during the typhoon season from May to September. Because the concentration of precipitation often induces natural disasters, such as severe landslides and debris flow, a quantitative assessment of sediment yielding caused by landslides is crucial for catchment management and debris flow prevention. An investigation of natural disasters cannot be conducted on-site because of terrain being unapproachable, the remoteness of an area, landslides in mountainous areas, or disaster-induced road closures. Research has only ever been able to be conducted through field surveys or conventional methods of remote sensing to obtain images of the site. With the progress of technologies associated with unmanned aerial vehicles (UAVs) or unmanned aircraft systems (UASs), image resolution and quality have considerably improved (Huang and Chang, 2014; Chen et al., 2015; Fernandez-Galarreta et al., 2015; Giordan et al., 2015; Tokarczyk, 2015; Deffontaines et al., 2016). Such technologies are capable of proving a wide range of image data on areas that humans cannot reach. Finer than aerial images captured by traditional aircrafts, those captured by cameras mounted on UAV/UAS can be used to construct multi-temporal high-resolution digital terrain models (DTMs) for comparing topographical changes at various periods. This study employed a UAV to aerially photograph regions inaccessible to humans or mountain areas. Computer software was used to establish DTMs based on the aerial photographs captured at various periods; a comparison of these DTMs would be able to track sediment yields from landslides as well as sediment outflow from catchments. The changes in environment and disaster assessment were analyzed to formulate appropriate prevention measures for the entire catchment area.

2 STUDY AREA

This study involved exploration of Pu-tun-pu-nas Creek, located at the upper reach of the Laonung River basin in southern Taiwan (Fig. 1), which is one of the numerous tributaries upstream of the Laonung River. Although its contributing area only accounts for approximately 1% of the total contributing area above the confluence of the main tributaries, Pu-tun-pu-nas Creek has a contributing area in which landslide and debris-flow disasters occur the most frequently of all the tributaries. As a result, a large amount of sediment supplies from Pu-tun-pu-nas Creek flow into the main channel of the Laonung River and significantly affect its topographic variation (Capart et al., 2010). The contributing areas of the Pu-tun-pu-nas Creek is approximately 7 km^2, and the river length is 4.8 km. Furthermore, the elevation ranges from 603 to 2,143 m, the average slope gradient of whole area is 31°, and the average slope gradient of the mainstream channel is 16.5°. In addition to the relatively weak lithology in this area, the Kaochung and Tulungwan faults under the river might cause landslide and debris-flow disasters whenever heavy rain occurs. Regarding the types of stratum exposure, the middle–upper reach of the catchment is composed of thick-bedded and muddy sandstone; the middle–lower reach of the catchment primarily consists of alternations of sandstone and shales; confluence of the main tributaries at the downstream reach (i.e., catchment outlet) contains argillite and/or slate intercalated with sandstone lentils and mixed with gravel, sand, and clay. In 2009, typhoon Morakot brought an astounding amount of rainfall in southern and eastern Taiwan. The rainfall data from the Hsinfa Rainfall Station of the Central Weather Bureau, Taiwan, indicated a rainfall duration of 70 hours and a total accumulated precipitation of 2,425 mm. Both the 24-hour and 48-hour accumulated rainfall data exceeded the recurrence interval of 200 years (Tseng et al., 2013). Precipitation characteristics of high intensity and long

duration result in numerous new landslides of the study area, in which the landslide area increased from 111 hectares to 319 hectares after typhoon Morakot, approximately three times that of the original area. Additionally, a largescale alluvial fan was created from debris flow formed at the confluence for the main tributaries of the downstream reach (Fig. 2). Since the arrival of typhoon Morakot, within the study area, sediment yields have been in great quantity and transport have been extremely active. When confronted with heavy rainfall, old landslide areas continues to enlarge as well as new landslides occur that serve as the source debris flow.

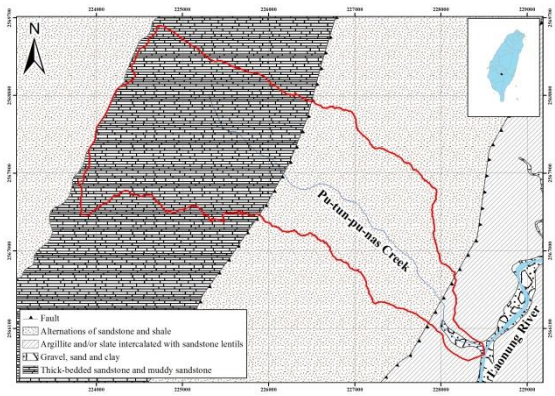

Figure 1. Geological map of the study area. The bold red shows the boundary line of Pu-Tun-pu-nas Creek basin

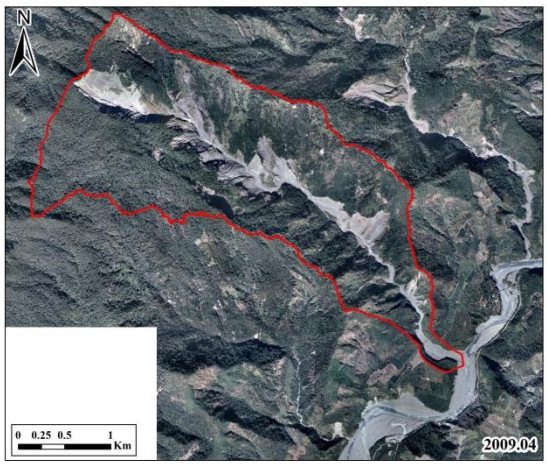

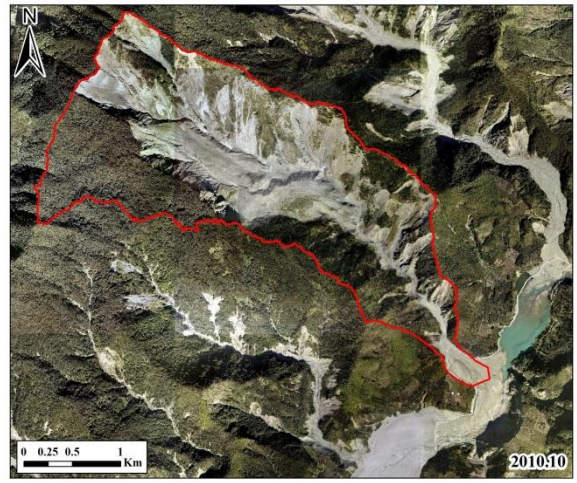

Figure 2. Landslides areas before and after typhoon Morakot

3 TOPOGRAPHY DATA ACQUISITION

This study used a camera mounted on a UAV to capture images of slopes and channels in a catchment for constructing DTMs, the main objective being to analyze sediment yields from landslides and sediment transport of the study area at different periods. Being unmanned and autopilot, a UAV is characterized by the benefits of low cost, convenience, and high resolution, all of which facilitate various aspects of its application. This study integrated Skywalker X8 UAV with the Ardupilot Mega 2.6 autopilot system (Chang et al., 2018) for data collection. A Sony ILCE-QX1 camera was mounted on the UAV. The duration for a single trip was approximately 90–120 min, with a speed of approximately 10–15 m/s. Pix4Dmapper, photogrammetry software was employed to construct DTMs of various periods. ArcGIS software was used to analyze and calculate variations among river channels based on these DTMs. The procedures for constructing DTMs were as follows: 1. import of basic parameters; 2. initialization; 3. point cloud densification; and 4. generation of the digital surface model (DSM) and orthorectified image. DSM (Fig. 3) were obtained from the interpolation of the encrypted

point cloud, and each image underwent tilt and height corrections before being spliced together to produce an integral orthorectified image (Fig. 4).

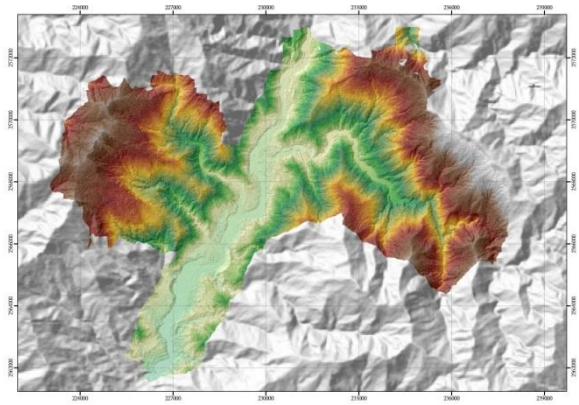

Figure 3. Digital surface model generated by the UAV photos

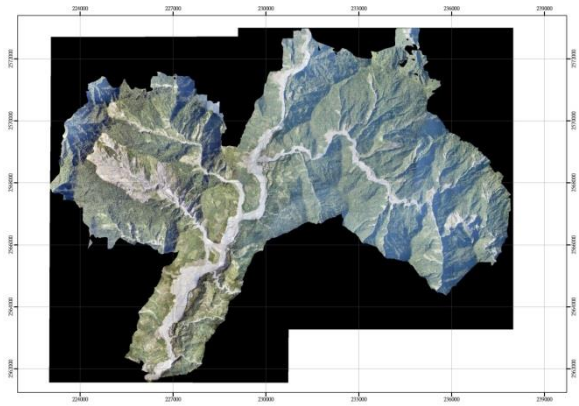

Figure 4. Orthomosaic image generated by the UAV photos

4 RESULTS AND DISCUSSIONS

4.1 Multi-temporal DTMs and accuracy evaluation

This study involved the construction of a DTM and orthorectified image of three periods. DTM data and images were from the following three sources: light detection and ranging (LiDAR)-derived DSM or digital elevation models (DEM) in 2010; aerial images captured by an ADS40 Airborne digital sensor in July, 2012, and photographic images captured by the UAV in January and November of 2015. The time of imaging and the resolution of each image are presented in Table 1, in which models and image resolutions based on the UAV are superior to those of the other two. LiDAR-derived DTM constructed in 2010 were validated through comparison with ground-based differential global positioning system data; the vertical elevation error in flat areas was less than 0.3 m (Lin et al. 2013). The quality of multi-temporal photogrammetry generated DTMs should be evaluated before the data of different periods were compared to determine topographical variation. This study selected five fixed road sections from aerial photographs of each period, and 50 points were selected from each location. Elevation data were extracted from the DSMs that were based on orthorectified images captured with the ADS40 and UAV for comparison with LiDAR topography data; the results of the error evaluation were listed in Table 1, in which the average elevation error of the five road locations was approximately −0.03 to −0.25 m and the range of standard deviation (SD) was 0.21 to 0.35 m. With a possible error set at mean value ± 1 SD, the possible error for the elevation of the study area would range from −0.57 to 0.18 m.

Table 1. Images dataset and accuracy evaluation results

Date	2012/07	2015/01	2015/11
Source	ADS40	UAV	UAV
Image resolution	15 cm	13 cm	13 cm
Terrain resolution	2 m	13 cm	13 cm
Average error	-0.25 m	-0.03 m	-0.22 m
S.D.	0.3 m	0.21 m	0.35 m

4.2 Evolution of landslide areas and corresponding sediment variation

The aforementioned DTMs established on the basis of photographic images of ADS and UAV were compared with the LiDAR-derived DEM in 2010, respectively. DTM values were subtracted from those of the preceding DTM to obtain changes in elevation of scouring and deposition (Tseng et al., 2013, Tseng et al., 2015). The obtained results revealed the variations in sediment yield and transport caused by the following events: the torrential rainfall in June 12, 2012, typhoon Kong-Rey in 2013, and typhoon Soudelor in 2015. Fig. 5–Fig. 7 present the elevation differences between ADS40 topography in 2012, UAV topography in January 2015, and UAV topography in November 2015, respectively, with LiDAR topography in 2010 of the study area. The warm colors (i.e., red and yellow) indicate that the terrain elevation of later periods is lower than those of the earlier periods, reflecting the areas that have undergone slope failure or channel erosion; blue–purple colors signify that the terrain elevation in later periods is higher than those of the earlier periods, indicating areas of residual soil on the slope toes or channel deposition. After torrential rainfall in June 12, 2012, the catchment of Pu-tun-pu-nas Creek yielded a considerable amount of sediment from hillslope, among which the largest landslide area was approximately 45 hectares, as well as a sediment deposition in the main channel of Pu-tun-pu-nas Creek. Furthermore, a new flow path was created on the southern side of the old alluvial fan (Fig. 5). Since the occurrence of typhoon Kong-Rey in 2013, the landslide of sloping land has continued to expand in the Pu-tun-pu-nas Creek catchment area as well as in the lands of the left bank on the upper reach of the mainstream and on the south side of the channel head. The main stream of Pu-tun-pu-nas Creek also continues to deposit and the scouring on the southern side of the downstream alluvial fan exhibits a widening trend (Fig. 6). After the occurrence of typhoon Soudelor in 2015, the evolution in the landslide land of the Pu-tun-pu-nas Creek catchment has been nonsignificant. Only a section of the old landslide at the source of the northern side of the main stream has expanded, and a portion of the south side of the landslide has continued to grow. A portion of deposited sediment on the landslide site in the previous period had gradually moved downward. The main channel of Pu-tun-pu-nas Creek also exhibited a tendency toward deposition, with the scale of deposition at the outlet of the new flow path created on the southern side of the old alluvial fan exhibiting a slight reduction (Fig. 7). Fig. 8 displays the variation in the longitudinal profile of the landslide area on the south side upstream of the Pu-tun-pu-nas Creek catchment area from the occurrence of typhoon Morakot in 2009 to 2015, clearly exhibiting continual expansion of landslide scar.

The variation in the amount of sediment between the two periods of DTM was further analyzed in this study. Sediment variation can be differentiated into the amount of sediment yielding on the slope within the landslide area, the residual amount on the slope, and the amount of erosion and deposition in the channel. The grid areas of DTMs were multiplied by their erosion depth (negative value) or deposition depth (positive value) to obtain the erosion or deposition volume of various grids. Erosion and deposition volume can be ascertained by separately calculating of the landslide area and channel , respectively (Tseng et al., 2013, Tseng et al., 2015). Through this method of analysis, the variation in sediment volume among the three periods was determined. The Pu-tun-pu-nas Creek catchment has continued to undergo a large amount of sediment erosion since the invasion of typhoon Morakot in 2009. By comparing the July 2012 DTM with the 2010 LiDAR-derived DTM revealed that erosion from slope failure reached 20,772,000 m^3 and the deposition volume of slope failure was 1,498,000 m^3. The 2010 LiDAR-derived DTM

coupled with the January 2015 UAV DTM revealed that the erosion of slope failure reached 31,479,000 m³ and the deposition volume of slope failure reduced slightly to 1,370,000 m³. The 2010 LiDAR-derived DTM combined with the January 2015 UAV DTM revealed that the erosion from slope failure reached 35,572,000 m³, and the deposition volume of slope failure slightly increased to 1,892,000 m³. The integration of the 2010 LiDAR-derived DTM with the July 2012 DTM within the channel revealed that the volume of channel erosion was 164,000 m³ and of channel deposition reached 2,208,000 m³. The combination of the 2010 LiDAR-derived DTM and the January 2015 UAV DTM revealed that the channel-erosion volume decreased slightly to 126,000 m³, whereas the channel-deposition volume gradually increased to 28,910 m³. Comparing the results from the 2010 LiDAR-derived DTM and the November 2015 UAV DTM revealed that the channel-erosion volume increased slightly to 137,000 m³ and the channel-deposition volume slightly increased to 2,905,000 m³.

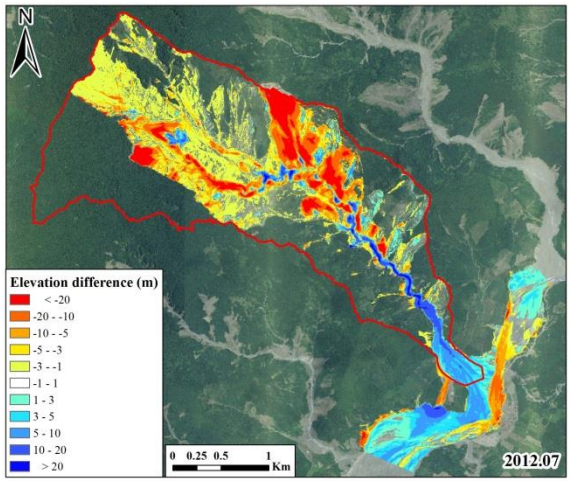

Figure 5. The elevation differences between 2012 ADS DSM and 2010 LiDAR DEM

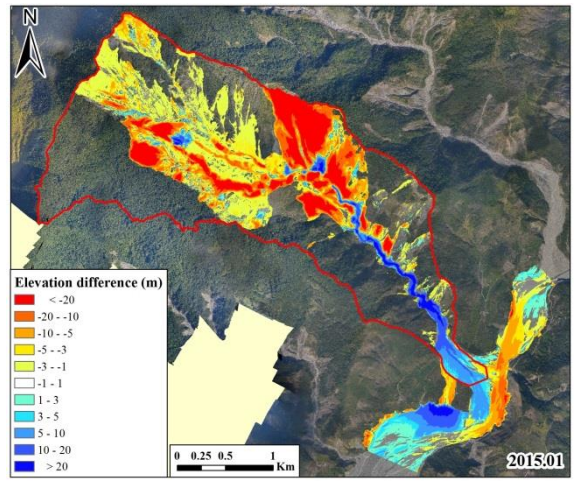

Figure 6. The elevation differences between 2015/01 UAV DSM and 2010 LiDAR DEM

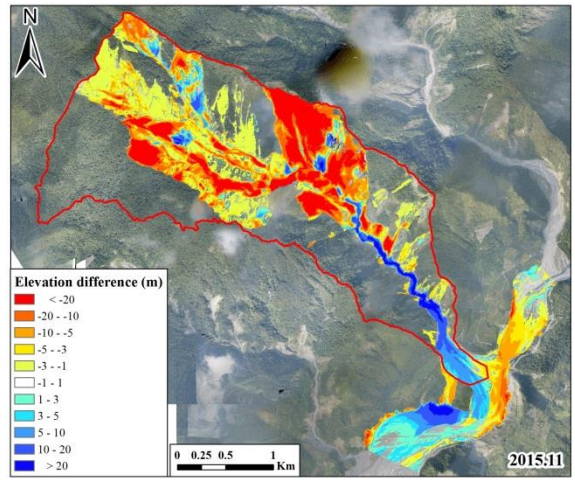

Figure 7. The elevation differences between 2015/11 UAV DSM and 2010 LiDAR DEM

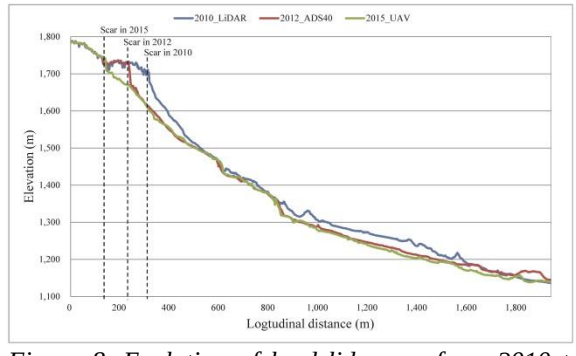

Figure 8. Evolution of landslide scar from 2010 to 2015

4.3 Variation of sediment outflow of the catchment

On the basis of the concept of the conservation of mass, the sediment outflux of the catchment between two DTMs period was calculated by adding the sediment erosion volume of the slope in the catchment to that of the channel and then subtracting the residual volumes and channel-deposition volumes (Tseng et al., 2017). Fig. 9 presents the variation from 2010, after the occurrence of typhoon Morakot, to November 2015 in the accumulated sediment outflow volume in the Pu-tun-pu-nas Creek catchment. The sediment outflow volume in the Pu-tun-pu-nas Creek catchment reached 30,912,000 m³. A comparison among the three DTMs indicated that torrential rainfall in June 12, 2012, generated a relatively large amount of sediment outflow; the volume of sediment outflow has gradually decreased since 2013. The sediment transport in the channel of the Pu-tun-pu-nas Creek catchment was primarily induced by debris flow. The formation of debris flow requires three fundamental conditions, namely sufficient water amount, channel gradient, and loose sediment provision, among which the channel gradient is extremely steep (16.5°), as described. The provision of landslide-derived sediment has been sufficient since the occurrence of typhoon Morakot in 2009. Any rainfall event that brings several hundred millimeters of precipitation may induce debris flow, which actively transports sediment yields from the upstream slope in the catchment to the main channel of the Laonung River. Fig. 9 showed sediment-transport capacity is generally positively correlated with the accumulated precipitation of rainfall events.

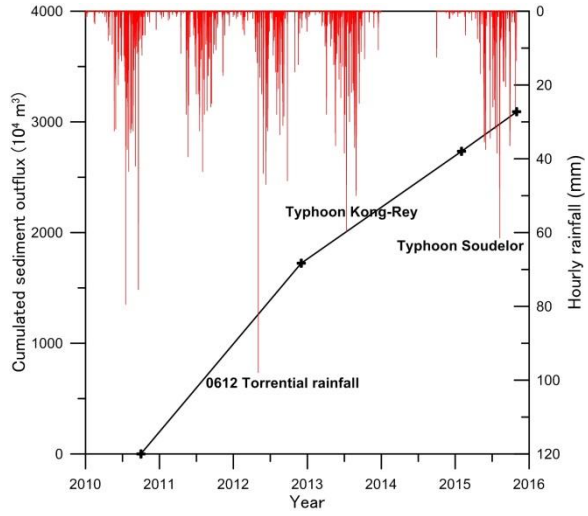

Figure 9. Temporal variation of the accumulated sediment outflux from 2010 to 2015

5 CONCLUSIONS

This study used aerial images captured by an ADS40 and UAV to construct several DTMs. By integrating an LiDAR-derived DTM, a total of four DTM periods were established to track the sediments yielded by landslides and sediment outflow by debris flow in the Pu-tun-pu-nas Creek catchment from the time that typhoon Morakot occurred in 2009 to the end of 2015 (a total of 6 years). After comparing with LiDAR digital terrain data to estimate the error of elevation in the fixed region of roads, the possible error range for elevation of the three-period DSM was determined to be approximatively −0.57 to 0.18 m. A comparison and analysis of the digital terrain data for four periods revealed that since the occurrence of typhoon Morakot in 2009, sediment yields had been sufficient and sediment transport extremely active within the Pu-tun-pu-nas Creek catchment, producing a substantial effect on the landform of the alluvial fan at the confluence of the main tributaries. This study revealed that the combination of multi-scale and multi-temporal digital terrain data enabled long-term tracking of sediment variation at the primary sediment-

yielding regions of remote locations inaccessible to humans. The obtained results are conducive for achieving further understanding of the physical mechanism of sediment yield and transport and, meanwhile, serve as an essential reference for the practical application of formulating a comprehensive disaster prevention and control strategy suitable for the basin.

6 ACKNOWLEDGEMENTS

This work is funded by the Soil and Water Conservation Bureau, Taiwan, R.O.C. and by the grant MOST 107-2625-M-309-003 from the Ministry of Science and Technology, Taiwan, R.O.C.

7 REFERENCES

Capart, H., Hsu, J.P.C., Lai, S.Y.J., Hsieh M.L. 2010. Formation and decay of a tributary-dammed lake, Laonong River, Taiwan, *Water Resour. Res.*, **46**, W11522.

Chang, K.J., Chan, Y.C., Chen, R.F., Hsieh, Y.C. 2018. Geomorphological evolution of landslides near an active normal fault in northern Taiwan, as revealed by lidar and unmanned aircraft system data, *Nat. Hazards Earth Syst. Sci.*, **18**, 709–727.

Chen, J., Li, K., Chang, K.J., Sofia, G., Tarolli, P. 2015. Open-pit mining geomorphic feature characterization, *Int. J. Appl. Earth. Obs.*, **42**, 76–86.

Deffontaines, B., Chang, K.J., Champenois, J., Fruneau, B., Pathier, E., Hu, J.C., Lu, S.T., Liu, Y.C. 2016. Active interseismic shallow deformation of the Pingting terraces (Longitudinal Valley – Eastern Taiwan) from UAV high-resolution topographic data combined with InSAR time series, *Geomat. Nat. Haz. Risk.*, **8**, 120–136.

Fernandez-Galarreta, J., Kerle, N., Gerke, M. 2015. UAV-based urban structural damage assessment using object-based image analysis and semantic reasoning, *Nat. Hazards Earth Syst. Sci.*, **15**, 1087–1101.

Giordan, D., Manconi, A., Facello, A., Baldo, M., dell'Anese, F., Allasia, P., Dutto, F. 2015. Brief Communication: The use of an unmanned aerial vehicle in a rockfall emergency scenario, *Nat. Hazards Earth Syst. Sci.*, **15**, 163–169.

Huang, M.J., Chang, K.J. 2014. Unmanned Aerial Vehicle (UAV) associated DTM quality evaluation and application, *Mag. Chinese Inst. Civil Hydraulic Eng.*, **41**, 52–58 (in Chinese with English abstract).

Lin, C.W., Tseng, C.M., Tseng, Y.H., Fei, L.Y., Hsieh, Y.C., Tarolli, P. 2013. Recognition of large scale deep-seated landslides in forest areas of Taiwan using high resolution topography, *Journal of Asian Earth Sciences*, **62**, 389-400.

Tokarczyk, P., Leitao, J.P., Rieckermann, J., Schindler, K., Blumensaat, F. 2015. High-quality observation of surface imperviousness for urban runoff modelling using UAV imagery, *Hydrol. Earth Syst. Sci.*, **19**, 4215–4228.

Tseng, C.M., Lin, C.W., Stark, C.P., Liu, J.K., Fei, L.Y., Hsieh, Y.C. 2013. Application of a Multi-temporal, LiDAR-derived, Digital Terrain Model in a Landslide-Volume Estimation, *Earth Surface Processes and Landforms*, **38(13)**, 1587-1601.

Tseng, C.M., Lin, C.W., Chang, K.J. 2015. The Sediment Budgets Evaluation in a Basin Using LiDAR DTMs, *Engineering Geology for Society and Territory – Volume 3 River Basins, Reservoir Sedimentation and Water Resources*, Springer International Publishing Switzerland.

Tseng, C.M., Chang, K.J., Tarolli, P. 2017. The Sediment Production and Transportation in a Mountainous Reservoir Watershed, Southern Taiwan, *Advancing Culture of Living with Landslides - Volume 5 Landslides in Different Environments*, Springer International Publishing AG.